Third-order nonlinearity in Ge–Sb–Se glasses at mid-infrared wavelengths

Liyan Chen, Feifei Chen, Shixun Dai, Guangming Tao, Lihe Yan, Xiang Shen, Hongli Ma, Xianghua Zhang, Yinsheng Xu

Third-order nonlinearity in Ge-Sb-Se glasses at mid-infrared wavelengths

Liyan Chen[a], Feifei Chen[a], Shixun Dai[a], Guangming Tao[b], Lihe Yan[c], Xiang Shen[a], Hongli Ma[d], Xianghua Zhang[d], and Yinsheng Xu[a, *]

xuyinsheng@nbu.edu.cn

[a] *Laboratory of Infrared Materials and Devices, The Research Institute of Advanced Technologies, Ningbo University, Ningbo 315211, China*

[b] *CREOL, The College of Optics & Photonics, University of Central Florida, Orlando, Florida 32816, United States*

[c] *School of Electronics & Information Engineering, Xi'an Jiaotong University, No. 28, Xianning West Road, Xi'an, 710049, China*

[d] *Laboratory of Glass and Ceramics, UMR CNRS 6226, University of Rennes I, 35042 Rennes Cedex, France*

[*] Corresponding Author. Tel.: +86 574 8760 9870.

Graphical abstract

The nonlinearity of Ge-Sb-Se glasses at mid-infrared wavelengths are researched by Z-Scan technique and the large FOM (> 10) of $Ge_{20}Sb_{10}Se_{70}$ glass shows the greatest potential for mid-IR all optical switching devices.

Highlights

- The nonlinearity properties of Ge-Sb-Se glasses at mid-IR were explored.
- The third order nonlinearity increased with the refractive index at 1550 nm.
- The highest n_2 is found at 2000 nm.
- FOM of $Ge_{20}Sb_{10}Se_{70}$ glass is larger than 10 at mid-IR wavelengths.

Abstract: The optical properties of Ge-Sb-Se glasses have been extensively studied at telecom wavelengths in recent years. However, the understanding of nonlinearity in Ge-Sb-Se glasses at mid-infrared wavelengths still remains limited. In this work, a series of $Ge_{20}Sb_xSe_{80-x}$ (x=0, 5, 10) glasses were prepared by conventional melt–quenching method. The absorption spectra and the refractive index of glasses were recorded. The third order nonlinearity, n_2, and nonlinear absorption coefficient were measured for Ge-Sb-Se glass samples at the wavelengths of 1550, 2000 and 2500 nm by Z-scan technique, respectively. With the increasing of Sb contents, the linear refractive index of glass increased. Among the three operating wavelengths, all the three glass samples have a highest n_2 at 2000 nm. By using the figure of merit (FOM) to evaluate the studied three glasses, the $Ge_{20}Sb_{10}Se_{70}$ glass shows the greatest potential for mid-IR all optical switching devices.

Keywords: chalcogenide; glass; nonlinear optics; optical materials;

1. Introduction

All-optical signal processing is seen as critical for future telecommunication networks to address the growing demand for network flexibility, low cost, energy consumption, etc. [1] To realize all-optical switching (AOS), materials with large Kerr nonlinearity, ultrafast response time, as well as low linear, and nonlinear losses are required. Typically, transparent glasses with large nonlinearity are excellent candidates for AOS [2, 3]. As well known, the presence of atoms with large polarizability (e.g. Sb atom) in the glass composition increases the nonlinear refractive index of the material. Gómez et al. have investigated five wavelengths between 1400-1600 nm and reported the n_2 of Sb_2O_3-$SbPO_4$ glass operating in the range 1.6–4.1×10^{-15} cm^2/W [4]. Compared with oxide glass, chalcogenide glasses possess some superior optical properties, such as high linear refractive index (2.0–3.0 at 1.55 μm), wide IR transmission window (from visible to 10-20 μm), large nonlinear refractive index (×100 – ×1000 of silica) and ultrafast optical response (~100 fs), which make them excellent candidates for the third-order nonlinear optical materials [5-9]. In the past few years, near-IR and short-wave IR nonlinear optical properties of chalcogenide glasses, namely, the nonlinear refraction index (n_2), have been extensively studied. Wang et al. have reported that n_2 of As_2S_3 at 1.25 μm and 1.55 μm is 3.0×10^{-17} m^2/W and 2.3×10^{-17} m^2/W, respectively [10]. However, the characterization of the nonlinear (NL) optical

absorption and NL refraction of chalcogenide glass has been limited to the wavelengths of visible or near-IR less than 1686 nm [11].

The multi-photon absorption (MPA) places a basic limitation on the efficiency of any high nonlinear refraction index (n_2) materials in AOS schemes based on an intensity dependent refractive index, especially the strong two-photon absorption (TPA) in chalcogenide glasses. At telecom wavelengths, relatively high peak intensity is usually demanded to initiate the third order Kerr nonlinearity, simultaneously lead to a strong TPA. As a result, the high Kerr nonlinearity and relatively weaker MPA beyond the TPA region come to a combination, which makes chalcogenide glasses highly promising for nonlinear applications at mid-IR wavelengths [10, 12]. The enormous research on the supercontinuum generation from near-IR to mid-IR also demands the nonlinear properties of chalcogenide glasses at mid-IR wavelengths.

Nonlinear refraction (NLR) and TPA coefficient can be measured by Z-scan technique [13], in which a sample is scanned near the focal region of a focused laser beam. With the sample is moved along the propagation direction of the laser beam (Z-axis), it consequently experiences a phase and intensity modulation, which can be observed in its transmittance measured as a function of the sample position (z). If all the transmitted light is measured, only TPA affects the Z-scan. In this case, it refers to as open-aperture Z-scan. If part of

the transmitted light is detected due to the presence of an aperture in front of the detector, both NLR and TPA indicate themselves on a so-called closed-aperture Z-scan. For the sake of getting the NLR index, the TPA value that is obtained from an open-aperture Z-scan must be taken into account in the closed aperture Z-scan modeling [14, 15].

This paper reports on the measurements of the third-order nonlinearity of a compositional series of Ge-Sb-Se chalcogenide glasses using the Z-scan technique at the wavelengths of 1550 nm, 2000 nm and 2500 nm, respectively. Values of nonlinear refractive index (n_2) and TPA or three-photon absorption coefficient (3PA) at corresponding wavelengths were obtained.

2. Experiment

In this experiment, a series of $Ge_{20}Sb_xSe_{80-x}$ (x=0, 5, 10) glasses were prepared by a conventional melt–quenching method in a vacuumed silica ampoule. The high purity raw materials, Ge (99.999%), Sb (99.999%), and Se (99.999%), were carefully weighed, transferred into quartz ampoules and sealed in a vacuum at 2×10^{-3} Pa. The quartz ampoules with the raw materials were heated in rocking furnaces at 950 ^{o}C for 12 h to ensure homogenization of the mixture. Then the ampoules were quenched in water. In order to reduce stress and improve optical homogeneity, the glasses were annealed at temperature 10 °C below glass transition temperature (T_g) for 2 h and cooled down with a rate of 10 °C/h to room temperature. Glass rods were obtained

from the ampoules and cut into discs of 1 mm and 0.5 mm. These were then polished for optical studies.

The linear refractive indices from 1.7 to 15 μm were measured using Metricon 2010 Prism Coupler with an accuracy of ±0.001, and the nonlinearities were measured with the Z-scan technique. Both of them were measured using the 1mm thick samples. In the process of Z-scan experiment, the optical parametric amplifier, which is pumped by an 800 nm Ti:sapphire laser producing ≈ 150 fs laser pulses at a repetition rate of 1 kHz, was tuned to operate at three wavelengths of 1550, 2000, and 2500 nm, and the incident energy of single laser pulse was kept at 128 ± 10 nJ. The measurements were repeated ten times at different places on the sample surface to minimize experimental error. To realize the technique, the laser beam was focused by a 12 cm focal distance lens. Besides, the sample which was fixed in a computer-controlled translation stage was to be scanned in the focus region along the beam propagation direction (Z-axis). Negative values of Z correspond to locations of the sample between the focusing lens and its focal plane. A photo detector with an adjustable aperture in front of the sample was placed in the far-field region. The aperture size with radius r_a is related to the linear aperture transmittance by

$$S=\left[1-\exp\left(-2r_a^2/w_a^2\right)\right], \tag{1}$$

with w_a denoting the beam radius at the aperture for very low incident power. A closed-aperture Z-scan experiment corresponds to S<1, which is employed for n_2 measurements, while S=1 is used for the determination of α_2 [16, 17].

The MPA coefficient and nonlinear refractive index n_2 are obtained by analyzing open- and closed-aperture measurements, respectively [18-20]. In the case of open-aperture detection, the detected signal shows a valley-only trace, which indicates the existence of nonlinear MPA, depending on the wavelengths. By contrast, when the detection is carried out with the presence of aperture, the detected signal has a peak-valley trace, depending on the strength of nonlinear refraction at the focal point. The normalized transmittance can be obtained by integrating the intensity I. The total time-integrated transmission for the open aperture is theoretically fitted with equations (2) and (3) obtained from the derivations for MPA coefficients by Sutherland et al [12].

$$T_{\text{open}}(z) = -\frac{1}{2\sqrt{2}} \frac{\beta I_0 L_{eff}}{1 + \left(z / z_0 \right)^2} \tag{2}$$

where z is the longitudinal scan distance from the focal point of a Gaussian beam with an on-axis peak intensity of I_0 and z_0 is the confocal beam parameter; $L_{eff} = \alpha^{-1}\left(1 - e^{-\alpha L}\right)$ is the effective optical length, where α is the linear absorption coefficient for the samples and L is the sample thickness. For closed aperture z-scan a circular aperture with S<1 is placed behind the

sample, and the transmission is recorded as a function of z position. For small absorptive and refractive changes the transmissivity is given by,

$$T_{closed}(z) = 1 - \frac{8\pi}{\sqrt{2}\lambda} \frac{z/z_o (1-S)^{0.25} L_{eff} n_2 I_0}{\left[1+\left(z/z_0\right)^2\right]\left[9+\left(z/z_0\right)^2\right]} - \frac{1}{2\sqrt{2}} \frac{L_{eff}\beta I_0 \left[3-\left(z/z_0\right)^2\right]}{\left[1+\left(z/z_0\right)^2\right]\left[9+\left(z/z_0\right)^2\right]} \quad (3)$$

3. Results and discussion

As can be seen in Fig. 1, optical absorption spectra of Ge-Sb-Se glass samples (0.5 mm) were recorded from 500 nm to 2500 nm. We can find that the absorption edge λ_{vis}, defined as the absorption coefficient at 10 cm^{-1}, are 803, 811, 914 nm, respectively. With the glass content of Sb increasing from 0 to 10 mol. %, it moves to the longer wavelengths.

In the absorption spectrum of the glass, optical absorption in the ultraviolet region is decided by the intrinsic absorption of matrix inside, photon energy which is corresponded to the absorption edge is defined as the optical band gap [21, 22]. In recent years, optical band gap (E_g) of glasses has been considered having a great correlation with third-order nonlinear properties [23-25]. Related research results suggested that glasses with a narrower optical band gap usually have higher third-order nonlinear properties. Chen *et al*. have reported that in the glass network of Bi_2O_3-B_2O_3-BaO, weakening the B-O bands result in lowering optical band gap and enhancing third-order nonlinearity [26]. In addition, Xu *et al*. have studied third-order optical nonlinear characterizations of Bi_2O_3-B_2O_3-TiO_2 ternary glasses, and came to a

conclusion that n_2 decreases with the increasing of E_g in BBT_x (x = 1, 2, 3) glasses [27]. Here, E_g was obtained from ultraviolet absorption edge related to electron transition between conduction band and valence band with Tauc equation. To measure the optical band gap E_g, it is necessary to use relatively thin glass samples of 0.5 mm. According to the classical Tauc equation, E_g can be calculated through the absorption spectrum of the glass. Its expression is as follows,

$$\alpha h\upsilon = B(h\upsilon - E_g)^m \quad (4)$$

where α is the linear absorption coefficient, $h\upsilon$ is the incident photon energy, B is the electronic transition constant, exponent m is a parameter related to electron transition species caused by optical absorption. m=0.5 represents a direct allowed optical transitions (E_{dg}), while m=2 represents indirect allowed optical transitions (E_{ig}) [26, 28]. Figs. 2a and 2b describe E_{ig} and E_{dg} of the Ge-Sb-Se glass samples, respectively. Some information can be acquired directly from the experimental curves: with the Sb content increases from 0% to 10%, the value of E_{ig} decreases from 1.71 eV to 1.66 eV, and the value of E_{dg} decreases from 1.62 eV to 1.57 eV. According to the above conclusion, this behavior indicates that the $Ge_{20}Sb_{10}Se_{70}$ glass have the highest n_2 among these Ge-Sb-Se glass samples. The material parameters for the Ge-Sb-Se glass samples are summarized in Table I.

According to Miller's rule and Ref [11], the nonlinearity of one material can be estimated from the refractive index n_0 by following equation,

$$n_2 = 4.27 \times 10^{-16} \frac{\left(n_0^2 - 1\right)^4}{n_0^2} \ cm^2/W \qquad (5)$$

According to equation (5), the nonlinearity at different wavelengths can be estimated. Fig. 3 shows the dependence of refractive index n_0 and the nonlinear refractive index n_2 on the wavelength, respectively. Clearly, both of them decreased with increasing wavelength. However, the estimated tendency of the n_2 does not agree with the following results obtained by Z-scan technique.

When conducting the Z-scan experiment, the corresponding closed-aperture and open-aperture were executed at 1550 nm, 2000 nm, and 2500 nm, respectively. Typical closed-aperture (S=0.05) and open-aperture (S=1) Z-scan curves of the $Ge_{20}Sb_5Se_{75}$ are shown in Fig. 4, respectively. Due to very weak signal, the open-aperture Z-scan curve of $Ge_{20}Sb_5Se_{75}$ at 2500 nm cannot be obtained and is not shown here. As can be seen in Figs. 4a-c, the peak with a valley configuration manifests the self-defocusing behavior of the sample, namely, the positive value of nonlinear refraction. Meanwhile, the observed transmittance changes between the pre-focal ($Z<0$) minimum and the post-focal ($Z>0$) maximum in the closed Z-scan are due to the positive nonlinear indices of refraction of the samples [29, 30]. Further, it is evident that the $Ge_{20}Sb_5Se_{75}$ glass sample shows larger n_2 in terms of its larger

distance between peak and valley [14]. The gap between the normalized transmittance valley and the peak is largest in the curve of 2000 nm wavelength. The evident asymmetry between valley and peak in closed-aperture curve informed the presence of nonlinear absorption of the chalcogenide glasses, which was confirmed by the downward tendency of optical transmittance in the open-aperture Z-scans. The same behaviors were also observed in other samples.

The open-aperture Z-scan shown in Figs. 4d-e illustrates the intensity-dependent transmission of the $Ge_{20}Sb_5Se_{75}$. It can be seen that the optical transmission of the $Ge_{20}Sb_5Se_{75}$ shows a decreasing tendency as it approached the laser focus (z = 0), namely nonlinear absorption occurred as the laser density increased. At the MIR wavelengths of 2000 and 2500 nm, the most important experimental result found in open-aperture Z-scans is the presence of three-photon absorption (3PA) [31].

By fitting the curves with a classic procedure [18-20], the nonlinear refractive index, n_2, and the TPA (or 3PA) coefficient, α_2 (or α_3), of the three samples at 1550, 2000 and 2500 nm are calculated and listed in Table II, respectively. To ensure the accuracy of the measurements, the nonlinearity propertied of As_2Se_3 glass at 1550 nm was referred. We can find that with the increase of operating wavelength, the values of n_2 increase first and then decrease. The largest value of n_2 is found at 2000 nm for all the three samples.

From Table 1, the bandgap of the three glasses ranges from 1.71 to 1.66 eV for E_{ig} (or 1.62 to 1.57 eV for E_{dg}). For the present chalcogenides, the large 3PA at 2000 nm can be attributed to electron band-to-band transition type since $1/3E_g$ of the studied chalcogenide glasses is comparable to the hv at 2000 nm (hv = 0.62 eV) and smaller than it, thus n_2 behaviors of the chalcogenide glasses at 2000 nm is increased significantly when approaching to the 3PA resonance and the n_2 values are higher than those obtained from 1550 nm. As the wavelength goes to 2500 nm, as a result of the small photon energy (hv = 0.496 eV) that is below $1/3E_g$ of the three samples, therefore, origination of the 3PA at 2500 nm is defect absorption tail below the band gap, namely from Urbach absorption region. The weak Urbach type 3PA resulted in lower nonlinear refraction by the KK relations [18]; and consequently the smallest n_2 value among the three testing wavelengths.

Usually, figure of merit (FOM) is used to evaluate the performance of the nonlinear optical material. Since the main limitation of the chalcogenide glasses to be applied in AOS at mid-IR wavelengths is the TPA and 3PA, FOM can be expressed by $n_2/(\alpha_2\lambda)$ and $n_2/(\alpha_3\lambda I_0)$ (I_0 is the laser intensity at focus) for TPA and 3PA dominant materials, respectively. Normally, FOM>1 can be designed to the AOS devices while the FOM > 10 is ideal for efficient all-optical devices [32]. As presented in Table II, the FOMs at 2000 nm for $Ge_{20}Sb_{10}Se_{70}$ glass and at 2500 nm for $Ge_{20}Sb_5Se_{75}$ and $Ge_{20}Sb_{10}Se_{70}$ glasses

satisfy the criterion for all-optical devices (FOM > 10). Hence, the $Ge_{20}Sb_{10}Se_{70}$ can be selected for the mid-IR AOS devices.

4. Conclusions

In summary, we prepared a series of Ge-Sb-Se glass samples and investigated the TPA and third order nonlinearity at mid-IR wavelengths of 1550, 2000 and 2500 nm using Z-scan experiments with femtosecond laser pulses, respectively. With the increasing Sb contents, the linear refractive index increased. Among the three operating wavelengths, all the three glass samples have a highest n_2 at 2000 nm. By using the figure of merit (FOM) to evaluate the studied three glasses, the $Ge_{20}Sb_{10}Se_{70}$ glass shows the greatest potential for mid-IR all optical switching devices.

Acknowledgments

The Project Sponsored by the National Natural Science Foundation of China (Nos. 61205181, 61308094, 61377061), the State Key Program of National Natural Science of China (No. 61435009), Scientific Research Foundation for the Returned Overseas Chinese Scholars, State Education Ministry, and K. C. Wong Magna Fund in Ningbo University.

References

[1] M.D. Pelusi, F. Luan, E. Magi, M.R. Lamont, D.J. Moss, B.J. Eggleton, J.S. Sanghera, L.B. Shaw, I.D. Aggarwal, Opt. Express, 16 (2008) 11506-11512.

[2] K.B. Manjunatha, R. Dileep, G. Umesh, M.N. Satyanarayan, B. Ramachandra Bhat, Opt. Mater., 36 (2014) 1054-1059.

[3] A. Ajami, M.S. Rafique, N. Pucher, S. Bashir, W. Husinsky, R. Liska, R. Inführ, H. Lichtenegger, J. Stampfl, S. Lüftenegger, Proc. SPIE 7027, 15th International School on Quantum Electronics: Laser Physics and Applications, 70271H (December 19, 2008);

[4] L.A. Gómez, C.B. de Araújo, D. Messias, L. Misoguti, S. Zilio, M. Nalin, Y. Messaddeq, J. App. Phys., 100 (2006) 116105.

[5] R.W. Boyd, Academic Press, New York, 2008.

[6] A.A. Wilhelm, C. Boussard-Plédel, Q. Coulombier, J. Lucas, B. Bureau, P. Lucas, Adv. Mater., 19 (2007) 3796-3800.

[7] L. Calvez, H. Ma, J. Lucas, X. Zhang, Adv. Mater., 19 (2007) 129-132.

[8] Y.-S. Xu, J.-W. Cheng, J.-N. Qi, S.-S. Lu, K.-L. Lu, J.-W. Xu, Q.-F. Shao, S.-X. Dai, J. Inorg. Mater., 29 (2014) 735-740.

[9] W. Wei, R. Wang, X. Shen, L. Fang, L.D. Barry, J. Phys. Chem. C, 117 (2013) 16571-16576.

[10] T. Wang, V. Nalla, G. Jacek, Y. Cui, G. Qian, W. Ji, D.T. Tan, Opt. Express, 21 (2013) 32192-32198.

[11] T. Wang, X. Gai, W. Wei, R. Wang, Z. Yang, X. Shen, S. Madden, B. Luther-Davies, Opt. Mater. Express, 4 (2014) 1011-1022.

[12] A.D. Bristow, N. Rotenberg, H.M. Van Driel, Appl. Phys. Lett., 90 (2007) 191104-191104-191103.

[13] W.C. Hurlbut, Y.S. Lee, K.L. Vodopyanov, P.S. Kuo, M.M. Fejer, Opt. Lett., 32 (2007) 668-670.

[14] M. Yin, H. Li, S. Tang, W. Ji, Appl. Phys. B, 70 (2000) 587-591.

[15] S.V. Rao, N.K.M.N. Srinivas, D.N. Rao, L. Giribabu, B.G. Maiya, R. Philip, G.R. Kumar, Opt. Commun., 182 (2000) 255-264.

[16] S. Pramodini, Y.N. Sudhakar, M. Selvakumar, P. Poornesh, Laser Phys., 24 (2014) 045408.

[17] S. Pramodini, P. Poornesh, Opt. Laser Technol., 63 (2014) 114-119.

[18] M. Sheik-Bahae, A.A. Said, T.-H. Wei, D.J. Hagan, E.W.V. Stryland, IEEE J. Quantum Electron., 26 (1990) 760-769.

[19] M. Yin, H.P. Li, S.H. Tang, W. Ji, Appl. Phys. B, 70 (2000) 587-591.

[20] T. Wang, N. Venkatram, J. Gosciniak, Y. Cui, G. Qian, W. Ji, D.T.H. Tan, Opt. Express, 21 (2013) 32192-32198.

[21] E.S. Sazali, M.R. Sahar, S.K. Ghoshal, R. Arifin, M.S. Rohani, A. Awang, J. Alloys Compd., 607 (2014) 85-90.

[22] V. Ivanova, Y. Trifonova, P. Petkov, T. Petkova, Optoelectron. Adv. Mat., 8 (2014) 42-44.

[23] H. Ahn, M.T. Lee, Y.M. Chang, Appl. Phys. Lett., 104 (2014).

[24] I. Fuks-Janczarek, R. Miedzinski, M.G. Brik, A. Majchrowski, L.R. Jaroszewicz, I.V. Kityk, Solid State Sci., 27 (2014) 30-35.

[25] R. Bala, A. Agarwal, S. Sanghi, N. Singh, Opt. Mater., 36 (2013) 352-356.

[26] F. Chen, S. Dai, Q. Nie, T. Xu, X. Shen, X. Wang, Journal Wuhan University of Technology, Mater. Sci. Ed., 24 (2009) 716-720.

[27] T. Xu, F. Chen, S. Dai, N. Qiuhua, X. Shen, W. Xunsi, Physica B, 404 (2009) 2012-2015.

[28] F. Chen, B. Song, C. Lin, S. Dai, J. Cheng, J. Heo, Mater. Chem. Phys., 135 (2012) 73-79.

[29] F. Chen, T. Xu, S.X. Dai, Q. Nie, X. Shen, X. Wang, B. Song, J. Non-Cryst. Solids, 356 (2010) 2786-2789.

[30] X. Zheng, M. Feng, Z. Li, Y. Song, H. Zhan, J. Mater. Chem. C, 2 (2014) 4121-4125.

[31] B. Gu, J. Wang, J. Chen, Y.-X. Fan, J. Ding, H.-T. Wang, Opt. Express, 13 (2005) 9230-9234.

[32] A. Zakery, S.R. Elliott, Optical nonlinearities in chalcogenide glasses and their applications, Springer, 2007.

Figure captions

Fig. 1. Absorption spectra of Ge-Sb-Se glass samples.

Fig. 2. Indirect allowed optical band gap (a) and direct allowed optical band gap (b) of the Ge-Sb-Se glass samples, respectively.

Fig. 3. The dependence of refractive index n_0 (a) and the nonlinear refractive index n_2 (b) on the wavelength, respectively.

Fig. 4. Closed-aperture Z-scan curves (a-c) of $Ge_{20}Sb_5Se_{75}$ at 1550, 2000, and 2500 nm, respectively. Open-aperture Z-scan curves (d-e) of $Ge_{20}Sb_5Se_{75}$ at 1550 and 2000 nm, respectively.

Table I. Material parameters for the Ge-Sb-Se glass samples.

Samples	E_{ig} /eV	E_{dg} /eV	λ_{vis} /nm	T_g /°C	Density /g.cm^{-3}
$Ge_{20}Se_{80}$	1.71	1.62	803	163.7	4.47
$Ge_{20}Sb_5Se_{75}$	1.68	1.59	811	188.0	4.51
$Ge_{20}Sb_{10}Se_{70}$	1.66	1.57	914	216.5	4.63

Table II. n_2, α_2 and α_3 of the Ge-Sb-Se glass samples at 1550, 2000 and 2500 nm, respectively.

Samples	1500 nm			2000 nm			2500 nm		
	n_2 /10^{-18} m^2·W^{-1}	α_2 /10^{-13} m·W^{-1}	*FOM*	n_2 /10^{-18} m^2·W^{-1}	α_3 /10^{-27} m^3·W^{-2}	*FOM*	n_2 /10^{-18} m^2·W^{-1}	α_3 /10^{-27} m^3·W^{-2}	*FOM*
$Ge_{20}Se_{80}$	3.72	6.01	4	17.45	26.91	4	2.68	4.34	3.1
$Ge_{20}Sb_5Se_{75}$	4.29	3.14	8.8	16.56	31.82	3.3	2.78	<0.5	>10
$Ge_{20}Sb_{10}Se_{70}$	6.22	4.78	8.4	16.72	8.83	11.8	2.97	<0.5	>10
As_2Se_3	10	16	4	25	49	4.1	4.4	29.7	0.7

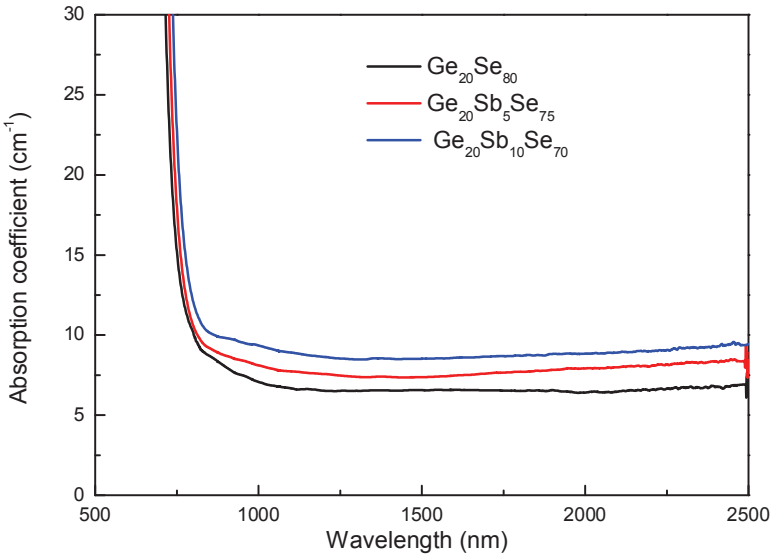

Fig. 1

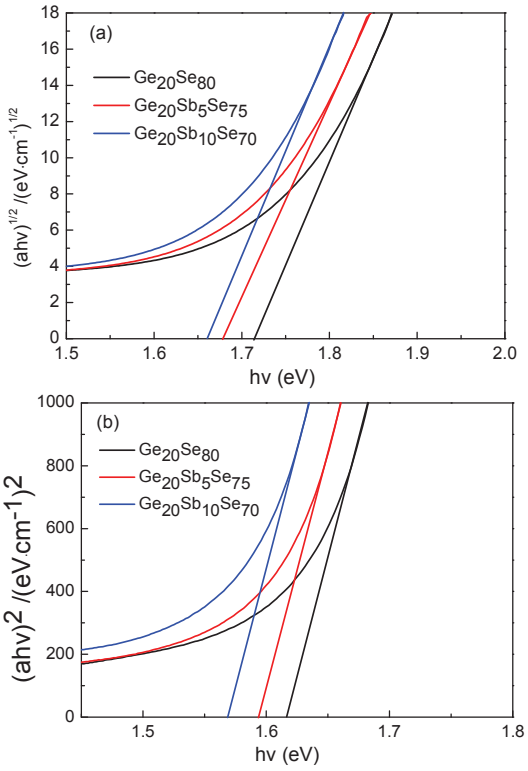

Fig. 2

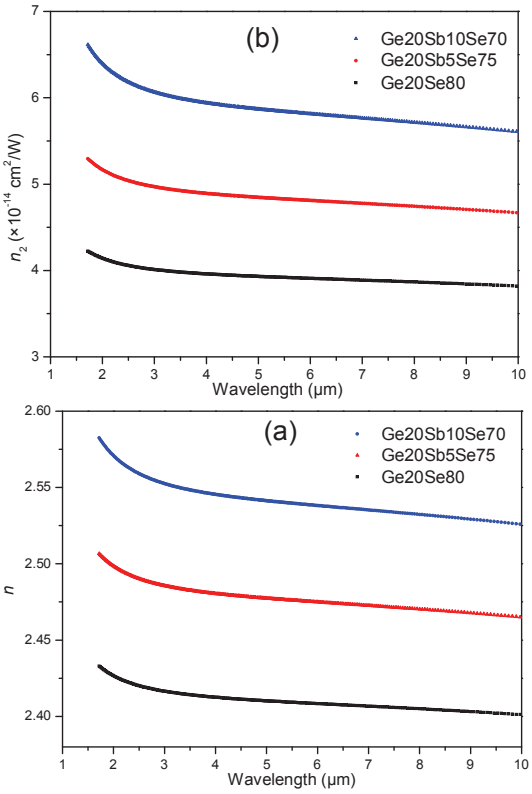

Fig. 3

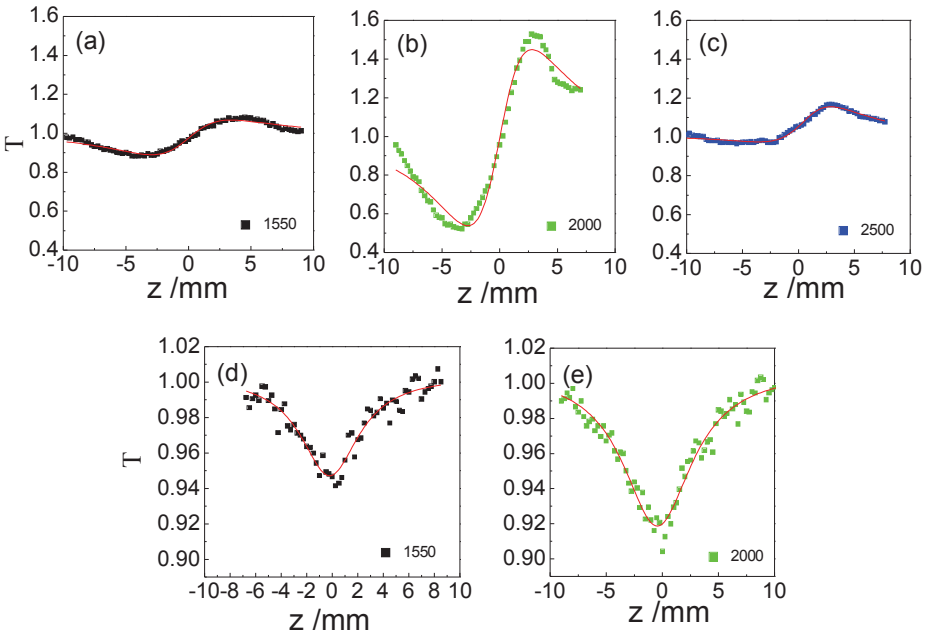

Fig. 4